Catalysis Science & Technology

ROYAL SOCIETY OF CHEMISTRY

PAPER

View Article Online
View Journal

Cite this: DOI: 10.1039/d6cy00561f

Shedding light on the copper-catalysed diboron(4) reduction of nitrous oxide

Thomas M. Hood, [a] Andrew C. C. Ward, [a] Tobias Krämer *[b] and Adrian B. Chaplin *[a]

Catalytic deoxygenation of the potent greenhouse gas and ozone-depleting agent N_2O mediated by NHC-ligated copper(I) boryl complexes has been examined under a variety of reaction conditions, including different diboron(4) reducing agents, and benchmarked against a rhodium(I) system. While unstable and decomposing rapidly in light, complexes of SIMes and IMes deliver the highest catalytic activity in combination with B_2pin_2 as the reducing agent when performed in the dark using THF as the solvent, achieving ~2000 TONs over 20 h at room temperature under 1 bar gauge of N_2O pressure. DFT-based computational analysis corroborates a mechanism involving reaction of the copper(I) boryl with N_2O by O-atom insertion into the Cu–B bond (*via* initial κ_N-coordinaton) followed by sigma-bond metathesis between the resulting boroxide derivative and diboron(4) reducing agent, with the relative barriers nuanced by the nature of the supporting NHC ligand and solvent employed.

Received 27th April 2026,
Accepted 26th May 2026

DOI: 10.1039/d6cy00561f

rsc.li/catalysis

Introduction

Nitrous oxide (laughing gas, N_2O) is the third most abundant greenhouse gas, with a global warming potential 273 times greater than carbon dioxide, and the dominant ozone depleting substance emitted in the 21st century.[1] Exponentially increasing anthropogenic emissions make it imperative that methods for the remediation and/or repurposing of nitrous oxide are developed, but controlled activation of this atmospheric pollutant has proven to be a challenging problem.[2] For homogeneous late transition metal complexes, insertion into covalent M–X bonds (X = H, C, B) has emerged as a promising strategy,[3] as exemplified by the use of ruthenium and rhodium hydride complexes as (pre-)catalysts for the hydrogenation of N_2O.[4] Building upon stoichiometric work by Braun using $[(Et_3P)_3Rh(Bpin)]$ (**1**, Scheme 1A),[5] and recognising the propensity of boron to form very strong bonds with oxygen (D_e = 809 kJ mol^{-1}),[6] we have recently set about investigating the use of late transition metal boryl complexes as homogeneous catalysts for the deoxygenation of N_2O.

In preceding work, carried out in collaboration with Liptrot and inspired by the homogeneous process developed by Sadighi for the reduction of isoelectronic CO_2,[7] we showed that NHC-ligated copper(I) *tert*-butoxide complexes are effective pre-catalysts for the deoxygenation of N_2O to N_2 using the diboron(4) compound B_2pin_2 (pin = pinacolato) as the reductant in benzene.[8] Robust catalytic performance was noted for [(SIPr)Cu(O*t*Bu)] **2*** and the proposed mechanism, involving reaction of the corresponding copper(I) boryl [(SIPr)Cu(Bpin)] **2** with N_2O by O-atom insertion into the Cu–B bond to liberate N_2 followed by rate determining sigma-bond metathesis between [(SIPr)Cu(OBpin)] **2′** and B_2pin_2, was established for this system experimentally (Scheme 1B). Guided by protocols reported in the literature,[7,9] all reactions were performed in the dark to mitigate against the inferred sensitivity of the catalytically active copper(I) boryls to light. Catalyst decomposition was however noted during initial catalyst screening, performed within high-pressure

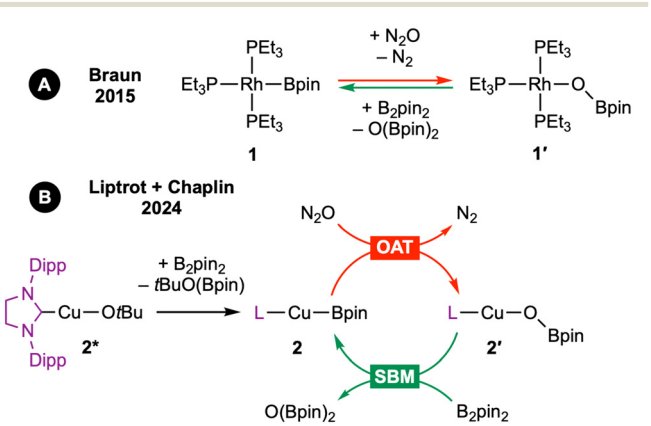

Scheme 1 (A) Stoichiometric and (B) catalytic deoxygenation of N_2O mediated by metal boryl complexes using B_2pin_2 as the reductant (pin = pinacolato).

[a] *Department of Chemistry, University of Warwick, Gibbet Hill Road, Coventry, CV4 7AL, UK. E-mail: a.b.chaplin@warwick.ac.uk*
[b] *School of Chemistry, Trinity College Dublin, The University of Dublin, Dublin 2, Ireland. E-mail: kraemert@tcd.ie*

J. Young value NMR tubes shielded from light (with foil when not in the spectrometer), particularly in the case of the Mes-substituted NHC systems examined. Productive photoactive copper(I) systems are typically tetracoordinated.[10]

Results and discussion

With a view of optimising the experimental conditions, the copper(I)-catalysed deoxygenation of N_2O was re-examined for a homologous series of *tert*-butoxide precatalysts, where the supporting NHC ligand is SIPr (**2***), IPr (**3***), SIMes (**4***), or IMes (**5***),[11] using commercially available B_2pin_2, B_2neop_2 (neop = neopentyl glycolato), or B_2cat_2 (cat = catecholato) as the diboron(4) reducing agent and THF or toluene as the solvent (Table 1A and B). Catalytic activity was assessed using 5 mol% pre-catalyst (5 mM) at room temperature under 1/3 bar gauge N_2O (1/3 bar absolute N_2O, balance argon) in the dark. Experiments were performed in parallel using a bespoke multiwell stainless-steel pressure reactor (Table 1C), with each individual reaction conducted within an amberised glass vessel that was charged with the pre-catalyst, diboron(4) and solvent in an argon filled glovebox in the dark to ensure the most rigorous exclusion of light possible. For comparison, the catalytic activity of unligated copper *tert*-butoxide **6*** and $[(Et_3P)_3Rh(OPh)]$ **1***[12] were determined under selected reaction conditions. Control experiments verified that, the diboron(4) reagents do not react with N_2O under the conditions studied.

This expanded catalyst screening reaffirms that NHC-ligated copper(I) *tert*-butoxide complexes are effective pre-catalysts for the deoxygenation of N_2O, using diboron(4) compounds as the reducing agent that afford bis(boryl)oxides as the boron-containing byproducts of the reaction (alongside boryl *tert*-butoxide, see SI). Using our refined protocol, the Mes-substituted NHC pre-catalysts **4*** and **5*** are found to the most active N_2O deoxygenation catalysts when using B_2pin_2 as the reducing agent and p_{N_2O} = 1 or 3 bar gauge, with complete consumption of diboron(4) observed in both THF and toluene within 2 h. Repeating these reactions under reduced turnover conditions revealed a N_2O pressure dependency in toluene, and enabled a lower activity limit of $TOF_{avg} > 40\ h^{-1}$ to be established. In combination with the less bulky alkyl diboron(4) B_2neop_2, these pre-catalysts do, however, show reduced activity and are outperformed by the Dipp-substituted NHC-precatalysts **2*** and **3*** (Table 1, entries 9 and 10), which are otherwise notable for enhanced activity in toluene with B_2pin_2. The copper(I) complexes are found to be least effective in catalysis when B_2cat_2 was used as the reducing agent and this outcome is attributed to detrimental reactions of the associated boryl derivatives initiated by Lewis acids (*e.g.* *t*BuO(Bcat), $O(Bcat)_2$).[13] In this context, it is interesting to note that the rhodium(I) pre-catalyst **1*** performs best in combination with B_2cat_2 and the associated deoxygenation activity ($TOF_{avg} \sim 9\ h^{-1}$) can be reproduced for pincer analogues of the form [Rh(pincer)X] (pincer = 2,6-(iPr$_2$PCH$_2$)$_2$C$_5$H$_3$N, X = OPh; Xantphos-*i*Pr, X = Bpin; see SI).[14]

Table 1 Catalyst screening for the diboron(4) reduction of N_2O[a]

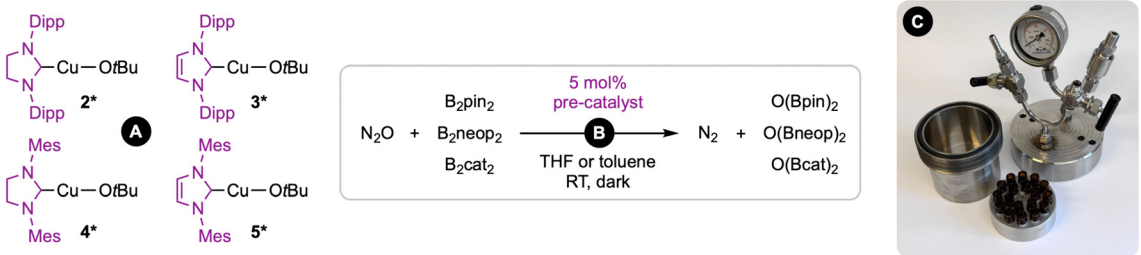

	Conditions				Conversion/%					
Entry	Diboron(4)	Solvent	p_{N_2O}/bar	Time/min	**1***	**2***	**3***	**4***	**5***	**6***
1	B_2pin_2	THF	3	120	6	34	87	100	100	22
2	B_2pin_2	THF	3	10				99	92	
3	B_2pin_2	THF	1	120		33	90	100	100	
4	B_2pin_2	THF	1	10				96	93	
5	B_2pin_2	Toluene	3	120		81	99	100	100	21
6	B_2pin_2	Toluene	3	10				58	84	
7	B_2pin_2	Toluene	1	120		81	100	100	100	
8	B_2pin_2	Toluene	1	10				42	63	
9	B_2neop_2	THF	3	120	35	77	83	52	63	12
10	B_2neop_2	Toluene	3	120		87	74	41	36	16
11	B_2cat_2	THF	3	120	88	25	29	<5	<5	0
12	B_2cat_2	Toluene	3	120		19	13	20	13	<5

[a] Conditions: 5 μmol precatalyst and 100 μmol of diboron(4) in 1 mL of solvent. Individual samples prepared in the dark within amberised glass vessels and parallel reactions run at room temperature inside a stainless-steel pressure reactor (1 atm argon, pressured to 1/3 bar gauge N_2O). Conversion determined by ^{11}B NMR spectroscopy and averaged over duplicate runs.

To help understand the influence of light in catalysis, we have systematically studied the stability of the copper(I) boryl complexes [(NHC)Cu(Bpin)] **2–5** (20 mM), generated *in situ* from reaction of the pre-catalysts [(NHC)Cu(O*t*Bu)] (**2***–**5***) with B_2pin_2 in THF and toluene, with and without precautions for the exclusion of light (Table 2). In our hands, the Dipp-substituted NHC boryls **2** and **3** are stable in the dark and undergo only slow decomposition when exposed to light, with [(SIPr)Cu(Bpin)] practically light stable when prepared in THF (Table 2, entry 3). While the less bulky Mes-substituted NHC boryls **4** and **5** can be unambiguously identified *in situ* by ^{11}B NMR spectroscopy (*ca.* δ_{11B} 42) when prepared in the dark, both are unstable and decomposed extremely rapidly into an intractable mixture of species in the light. Overall, the stability of the boryl complexes decreases in the order **2** > **3** ≫ **4** > **5** and THF > toluene and these trends vindicate re-examining the catalytic activity of the copper pre-catalysts with more rigorous exclusion of light in different solvents. Running catalytic reactions under more dilute conditions, as we have here, may also lead to some discrepancies, as this would help suppress bimolecular catalyst decomposition pathways. Such processes will be more apparent at the relatively high copper concentrations used in this stability study to facilitate analysis by multinuclear NMR spectroscopy.

Given the large differences in light sensitivity evident for **2–5**, we turned to computational methods to interrogate the mechanistic subtleties in N_2O deoxygenation catalysis, focusing on the most effective diboron(4) reducing agent B_2pin_2 and selecting DFT calculations at the B3LYP-D3(BJ)/def2-TZVP//BP86-D3(BJ)/def2-SVP level of theory corrected for benzene, toluene or THF solvent (SMD).[15] Leveraging our preceding work in benzene as a robust experimental benchmark,[8] the reaction profile for SIPr-ligated **2** was analysed in the first instance. Particularly to assess the relative energetics of O-atom transfer pathways, involving concerted insertion into the Cu–B bond or, informed by related computational work,[16,17] addition of N_2O across the Cu–B bond (Fig. 1A). The former is associated with a prohibitively large barrier of $\Delta G^{\ddagger}_{298K}$ = 31.9 kcal mol^{-1} (**2**/TS_O) while two stepwise pathways for the latter, where the terminal O atom of N_2O approaches either the Cu ($\Delta G^{\ddagger}_{298K}$ = 18.9 kcal mol^{-1}, **2**/TS_{ON_2}) or B ($\Delta G^{\ddagger}_{298K}$ = 16.8 kcal mol^{-1}, **2**/TS_{N_2O}) centres, could be identified. The most favourable variant can be interpreted as a nucleophilic attack of the boryl at the pendant O atom of κ_N-coordinated N_2O, as can be visualised by EDA-NOCV analysis of associated transition state **2**/TS_{N_2O} (Fig. 1B).[18] Binding of N_2O along this pathway is substantiated by QTAIM analysis (Fig. S171) and, while endergonic in this case, there is experimental precedent for intact κ_N-coordinaton of N_2O to copper(I).[19]

The computed thermodynamics indicate that subsequent liberation of N_2 and formation of the resulting copper(I)-boroxide **2′** is highly exergonic, with ΔG_{298K} = −117.8 kcal mol^{-1} relative to **2** and N_2O. The onward sigma-bond metathesis step has previously been studied computationally by Lin and Mayer in the context of CO_2 reduction,[16] and the overall activation barrier ($\Delta G^{\ddagger}_{298K}$ = 21.3 kcal mol^{-1}, **2′**/TS_{SBM}) and thermodynamics (ΔG_{298K} = −5.4 kcal mol^{-1}, relative to **2** + B_2pin_2; *cf.* −123.2 kcal mol^{-1} for the overall transformation) at our chosen level of theory are in good agreement. Critically, the calculated activation barrier for this step is significantly larger than that of the O-atom transfer step ($\Delta\Delta G^{\ddagger}_{298K}$ = 4.5 kcal mol^{-1}), consistent with the experimental observation that this is rate determining (*viz.* no N_2O pressure dependence was observed during the screening).

Informed by this analysis, the activation barriers for the O-atom transfer and sigma-bond metathesis steps were computed for the complete homologous series of copper(I)-boryl catalysts **2–5**, as pertinent to the catalytic reactions performed in toluene and THF solvent (Table 3). O-atom transfer *via* TS_{N_2O} is most favourable for all systems (Table S6), with the calculated barriers for the Dipp-substituted NHC catalysts **2** and **3** marginally lower than the Mes-substituted analogues **4** and **5** ($\Delta\Delta G^{\ddagger}_{298K}$ *ca.* −2 kcal mol^{-1}, Table 3). Consistent with the relatively low activity observed for **2*** (Table 1, entries 1 and 5), rate determining sigma-bond metathesis between SIPr-ligated **2′** and B_2pin_2 invokes a barrier *ca.* 3 kcal mol^{-1} higher than for **3′–5′**. Moreover, the significantly higher activity observed for **2*** in toluene *vs.* THF is reproduced computationally. Higher barriers

Table 2 Stability of boryl derivatives **2–5** generated *in situ* from the reaction between [(NHC)Cu(O*t*Bu)] **2***–**5*** and B_2pin_2 at room temperature[a]

	Conditions		Stability [(NHC)Cu(Bpin)]			
Entry	Solvent	Light	**2** (SIPr)	**3** (IPr)	**4** (SIMes)	**5** (IMes)
1	THF	Dark	Stable	Stable	$t \sim 30$ min	$t < 10$ min
2	THF	Ambient	Stable	$t > 24$ h	$t < 10$ min	Not observed
3	THF	Direct sunlight	Stable	$t_{1/2} \sim 10$ h		
4	Toluene	Dark	Stable	Stable	$t \sim 30$ min	$t < 5$ min
5	Toluene	Ambient	Stable	$t > 24$ h	$t < 5$ min	Not observed
6	Toluene	Direct sunlight	$t > 24$ h	$t_{1/2} \sim 3$ h		

[a] Conditions: 10 μmol **2–5** and 11 μmol of B_2pin_2 in 0.5 mL of either d_8-THF or d_8-toluene. Samples prepared in the dark within either an amberised or clear glass J. Young valve NMR tube. Ambient = interior laboratory lighting, direct sunlight = placed adjacent to a window on a sunny day.

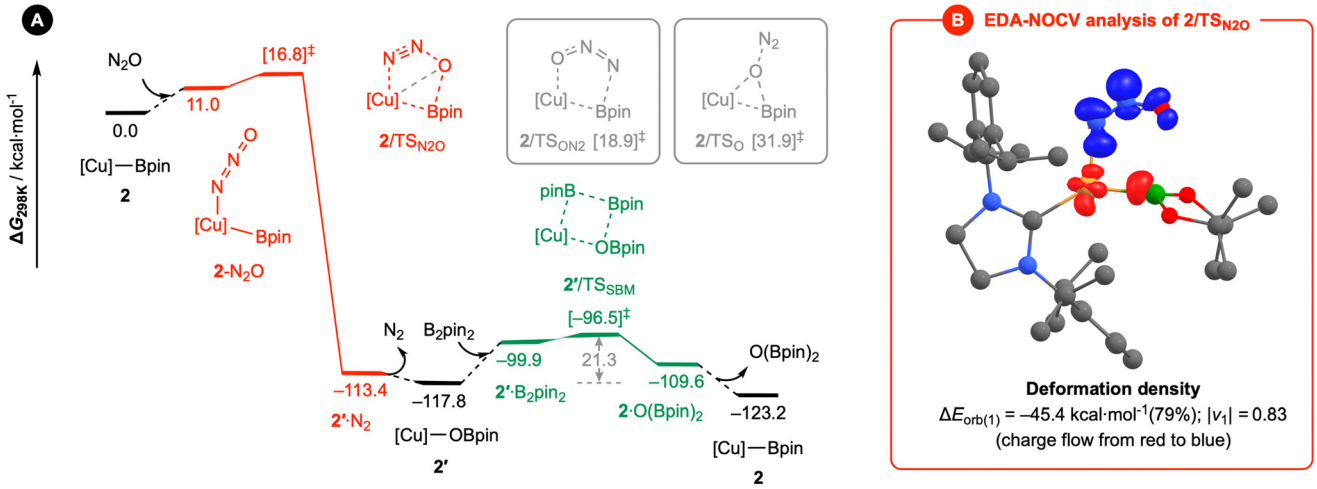

Fig. 1 (A) Computed reaction profile for deoxygenation of N_2O catalysed by **2** using B_2pin_2 as the reducing agent, with (B) EDA-NOCV analysis of the lowest energy O-atom transfer transition state. Calculations at the B3LYP-D3(BJ)/def2-TZVP//BP86-D3(BJ)/def2-SVP level of theory corrected for benzene solvent (SMD).[15]

for sigma-bond metathesis are calculated in THF *vs.* toluene across the board due to electrostatic stabilisation of the ground state in THF. Less pronounced solvent effects are found for the O-atom transfer barriers and has significant mechanistic implications for the Mes-substituted NHC catalysts **4** and **5**, for which the barriers for O-atom transfer and sigma bond metathesis in toluene are calculated to be within 0.5 kcal mol^{-1}, *cf.* the barrier for sigma-bond metathesis being >1 kcal mol^{-1} than O-atom transfer for **2** and **3** in toluene and **2–5** in THF. On this basis, the reduced catalytic activity and N_2O pressure dependency in toluene *vs.* THF observed experimentally for **4** and **5** is attributed to the deoxygenation of N_2O becoming a pseudo third order reaction in toluene.

Table 3 Calculated activation barriers $\Delta G^{\ddagger}_{298K}$/kcal mol^{-1} for the deoxygenation of N_2O catalysed by **2–5** using B_2pin_2 as the reducing agent

		THF			Toluene		
Catalyst	NHC	OAT	SBM	Δ	OAT	SBM	Δ
2	SIPr	16.0	23.0	7.0	16.7	21.2	4.5
3	IPr	16.4	19.9	3.5	17.0	18.4	1.4
4	SIMes	17.4	20.0	2.6	17.9	18.3	0.4
5	IMes	18.6	20.3	1.7	19.0	18.7	−0.3

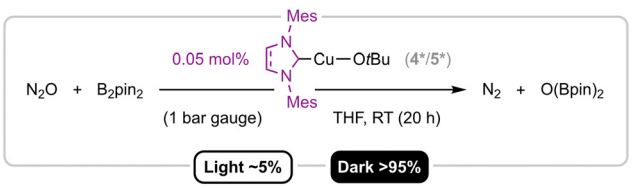

Scheme 2 High turnover conditions for the catalytic deoxygenation of N_2O.

Finally, to explore the limits of the Mes-substituted NHC copper complexes in N_2O deoxygenation catalysis, **4*** and **5*** were examined with a reduced catalyst loading of 0.05 mol% (0.05 mM) in combination with B_2pin_2 as the reducing agent and THF as the solvent at room temperature and p_{N_2O} = 1 bar gauge (Scheme 2). Under these mild conditions both pre-catalysts delivered >95% conversion after 20 h in the dark, corresponding to ~2000 TON and TOF_{avg} ~ 100 h^{-1}. This is a step-change in catalytic performance and productivity compared to our previous benchmarks of TON ~ 850 and TOF_{avg} ~ 35 h^{-1} set using **2*** at 80 °C.[8] Emphasising the importance of excluding light, only ~5% conversion was observed when these reactions were repeated in a glass pressure reactor exposed to ambient light throughout the experiment.

Conclusions

The catalytic deoxygenation of N_2O mediated by copper(I) complexes stabilised by Dipp- and Mes-substituted NHC ligands has been examined under a variety of reaction conditions, including different diboron(4) reducing agents, and benchmarked against a rhodium(I) system. While boryl derivatives are unstable and decompose rapidly in light, copper(I) pre-catalysts ligated by SIMes and IMes deliver the highest catalytic activity in combination with B_2pin_2 as the reducing agent when performed in the dark using THF as the solvent, achieving ~2000 TON over 20 h at room temperature under 1 bar gauge of N_2O pressure. DFT-based computational analysis of the copper(I)-boryl catalysed reaction corroborates a mechanism involving reaction with N_2O by O-atom insertion into the Cu–B bond (*via* initial κ_N-coordinaton) followed by sigma-bond metathesis between the resulting copper(I) boroxide and diboron(4) reducing agent,[20] with the relative barriers nuanced by the nature of the supporting ligand and solvent employed. These results further highlight

how late transition metal boryl complexes can be used as efficient catalysts for the transformation of N_2O and provide important insights into how the activity of copper(I) boryl systems, in general, can be optimised by careful consideration of the reaction conditions, especially the exclusion of light.

Conflicts of interest

There are no conflicts to declare.

Data availability

The data supporting this article have been included as part of the supplementary information (SI). Supplementary information: full experimental details and selected data; computational details and further analysis; optimised geometries in XYZ format. See DOI: https://doi.org/10.1039/d6cy00561f. CCDC 2549087 and 2549088 contain the supplementary crystallographic data for this paper.[21]

Acknowledgements

This work was supported by NERC grants NE/S007350/1 (CENTA2 studentship to ACCW) and NE/X018377/1. We also acknowledge funding from the Leverhulme Trust (RPG-2022-214, TMH) and the University of Warwick. Computational resources and technical support provided by DJEI/DES/SFI/HEA Irish Centre for High-End Computing (ICHEC) and LuxProvide.

References

1 A. R. Ravishankara, J. S. Daniel and R. W. Portmann, *Science*, 2009, **326**, 123–125; *Sixth Assessment Report from the IPCC*, 2021, https://www.ipcc.ch/report/ar6/wg1/, (retrieved 07/04/2026).

2 W. B. Tolman, *Angew. Chem., Int. Ed.*, 2010, **49**, 1018–1024; K. Severin, *Chem. Soc. Rev.*, 2015, **44**, 6375–6386; X. Wu, J. Du, Y. Gao, H. Wang, C. Zhang, R. Zhang, H. He, G. Lu and Z. Wu, *Chem. Soc. Rev.*, 2024, **53**, 8379–8423; A. Genoux and K. Severin, *Chem. Sci.*, 2024, **15**, 13605–13617.

3 G. A. Vaughan, P. B. Rupert and G. L. Hillhouse, *J. Am. Chem. Soc.*, 1987, **109**, 5538–5539; P. T. Matsunaga, G. L. Hillhouse and A. L. Rheingold, *J. Am. Chem. Soc.*, 1993, **115**, 2075–2077; A. W. Kaplan and R. G. Bergman, *Organometallics*, 1997, **16**, 1106–1108; A. W. Kaplan and R. G. Bergman, *Organometallics*, 1998, **17**, 5072–5085; J.-H. Lee, M. Pink, J. Tomaszewski, H. Fan and K. G. Caulton, *J. Am. Chem. Soc.*, 2007, **129**, 8706–8707; S. W. Kohl, L. Weiner, L. Schwartsburd, L. Konstantinovski, L. J. W. Shimon, Y. Ben-David, M. A. Iron and D. Milstein, *Science*, 2009, **324**, 74–77; D. J. Mindiola, L. A. Watson, K. Meyer and G. L. Hillhouse, *Organometallics*, 2014, **33**, 2760–2769; L. E. Doyle, W. E. Piers and J. Borau-Garcia, *J. Am. Chem. Soc.*, 2015, **137**, 2187–2190; F. L. Vaillant, A. M. Calbet, S. González-Pelayo, E. J. Reijerse, S. Ni, J. Busch and J. Cornella, *Nature*, 2022, **604**, 677–683; A. Mateos-Calbet, P. C. Bruzzese, M. A. Mermigki, A. Schnegg, D. A. Pantazis and J. Cornella, *J. Am. Chem. Soc.*, 2025, **147**, 19438–19443.

4 T. L. Gianetti, S. P. Annen, G. Santiso-Quinones, M. Reiher, M. Driess and H. Grützmacher, *Angew. Chem., Int. Ed.*, 2016, **55**, 1854–1858; R. Zeng, M. Feller, Y. Ben-David and D. Milstein, *J. Am. Chem. Soc.*, 2017, **139**, 5720–5723; I. Ortega-Lepe, P. Sánchez, L. L. Santos, P. Lara, N. Rendón, J. López-Serrano, V. Salazar-Pereda, E. Álvarez, M. Paneque and A. Suárez, *Inorg. Chem.*, 2022, **61**, 18590–18600; S. T. Nappen, J. J. Gamboa-Carballo, E. Tschanen, F. Ricatto, M. D. Wörle, A. Thomas, M. Trincado and H. Grützmacher, *Angew. Chem., Int. Ed.*, 2025, **64**, e202502616; S. H. Dewick, T. M. Hood, Y. Han, S. Huband and A. B. Chaplin, *Catal. Sci. Technol.*, 2025, **15**, 4126–4129.

5 S. I. Kalläne, T. Braun, M. Teltewskoi, B. Braun, R. Herrmann and R. Laubenstein, *Chem. Commun.*, 2015, **51**, 14613–14616.

6 Y. R. Luo, *Comprehensive Handbook of Chemical Bond Energies*, CRC Press, 2007.

7 D. S. Laitar, P. Müller and J. P. Sadighi, *J. Am. Chem. Soc.*, 2005, **127**, 17196–17197.

8 T. M. Hood, R. S. C. Charman, D. J. Liptrot and A. B. Chaplin, *Angew. Chem., Int. Ed.*, 2024, **63**, e202411692.

9 C. Borner, L. Anders, K. Brandhorst and C. Kleeberg, *Organometallics*, 2017, **36**, 4687–4690; W. Drescher, C. Borner and C. Kleeberg, *New J. Chem.*, 2021, **45**, 14957–14964; T. M. H. Downie, R. S. C. Charman, J. W. Hall, M. F. Mahon, J. P. Lowe and D. J. Liptrot, *Dalton Trans.*, 2021, **50**, 16336–16342.

10 J. Beaudelot, S. Oger, S. Peruško, T.-A. Phan, T. Teunens, C. Moucheron and G. Evano, *Chem. Rev.*, 2022, **122**, 16365–16609.

11 N. P. Mankad, D. S. Laitar and J. P. Sadighi, *Organometallics*, 2004, **23**, 3369–3371; D. S. Laitar, *PhD thesis*, Massachusetts Institute of Technology, USA, 2006, p. 43; G. G. Dubinina, J. Ogikubo and D. A. Vicic, *Organometallics*, 2008, **27**, 6233–6235; O. Santoro, F. Lazreg, Y. Minenkov, L. Cavallo and C. S. J. Cazin, *Dalton Trans.*, 2015, **44**, 18138–18144.

12 M. Teltewskoi, J. A. Panetier, S. A. Macgregor and T. Braun, *Angew. Chem., Int. Ed.*, 2010, **49**, 3947–3951.

13 W. Drescher and C. Kleeberg, *Inorg. Chem.*, 2019, **58**, 8215–8229.

14 M. A. Esteruelas, M. Oliván and A. Vélez, *Organometallics*, 2015, **34**, 1911–1924; J. J. Gair, Y. Qiu, N. H. Chan, A. S. Filatov and J. C. Lewis, *Organometallics*, 2017, **36**, 4699–4706.

15 S. H. Vosko, L. Wilk and M. Nusair, *Can. J. Phys.*, 1980, **58**, 1200–1211; J. P. Perdew, *Phys. Rev. B: Condens. Matter Mater. Phys.*, 1986, **33**, 8822–8824; C. Lee, W. Yang and R. G. Parr, *Phys. Rev. B: Condens. Matter Mater. Phys.*, 1988, **37**, 785–789; A. D. Becke, *Phys. Rev. A: At., Mol., Opt. Phys.*, 1988, **38**, 3098–3100; A. D. Becke, *J. Chem. Phys.*, 1993, **98**, 5648–5652; F. Weigend and R. Ahlrichs, *Phys. Chem. Chem. Phys.*, 2005, **7**, 3297–3305; F. Weigend, *Phys. Chem. Chem. Phys.*, 2006, **8**, 1057–1065; A. V. Marenich, C. J. Cramer and D. G. Truhlar, *J. Phys. Chem. B*, 2009, **113**, 6378–6396; S. Grimme, J. Antony, S. Ehrlich and H. Krieg, *J. Chem. Phys.*, 2010, **132**,

154104; S. Grimme, S. Ehrlich and L. Goerigk, *J. Comput. Chem.*, 2011, **32**, 1456–1465.
16 H. Zhao, Z. Lin and T. B. Marder, *J. Am. Chem. Soc.*, 2006, **128**, 15637–15643.
17 X. Guo and Z. Lin, *Chem. Sci.*, 2024, **15**, 3060–3070; X. Guo, T. Yang, F. K. Sheong and Z. Lin, *ACS Catal.*, 2021, **11**, 5061–5068.
18 T. Ziegler and A. Rauk, *Theor. Chim. Acta*, 1977, **46**, 1–10; A. Michalak, M. Mitoraj and T. Ziegler, *J. Phys. Chem. A*, 2008, **112**, 1933–1939; M. P. Mitoraj, A. Michalak and T. Ziegler, *J. Chem. Theory Comput.*, 2009, **5**, 962–975; L. Zhao, M. von Hopffgarten, D. M. Andrada and G. Frenking, *WIREs Comput. Mol. Sci.*, 2018, **8**, e1345.
19 V. Zhuravlev and P. J. Malinowski, *Angew. Chem., Int. Ed.*, 2018, **57**, 11697–11700.
20 Our computational analysis concurs with an independent study published during the preparation of this manuscript, F. Shiri and Z. Lin, *Inorg. Chem.*, 2026, **65**, 9617–9624.
21 CCDC 2549087: Experimental Crystal Structure Determination, 2026, DOI: 10.5517/ccdc.csd.cc2rkjmh; CCDC 2549088: Experimental Crystal Structure Determination, 2026, DOI: 10.5517/ccdc.csd.cc2rkjnj.

